Electronic supplementary information

A homoleptic tris(diphosphacyclobutadiene) tripledecker sandwich complex

Christian Rödl,[a] Gabriele Hierlmeier [a] and Robert Wolf [a]*

[a] *Universität Regensburg, Institut für Anorganische Chemie, 93040 Regensburg (Germany); E-Mail: robert.wolf@ur.de*

Content:

1 General Procedures

All experiments were performed under an atmosphere of dry argon using standard Schlenk techniques or a MBraun UniLab glovebox. Solvents were dried and degassed with a MBraun SPS800 solvent purification system. THF and toluene were stored over molecular sieves (3 Å). *n*-Hexane and *n*-pentane were stored over a potassium mirror. NMR spectra were recorded on an Avance 400 spectrometer at 300 K and internally referenced to residual solvent resonances. The UV/Vis spectrum was recorded on an Ocean Optics Flame Spectrometer. Mass spectrometry was performed by the analytical department of Regensburg University using a Jeol AccuTOF GCX. [Co($P_2C_2tBu_2SiMe_3$)($P_2C_2tBu_2$)] was synthesized according to the recently reported literature procedure.[1] [Cp*$RhCl_2$]$_2$ was purchased from Sigma Aldrich and used as received.

2 Synthesis of [Co_2(η^4-$P_2C_2tBu_2$)$_2$(μ:η^4:η^4-$P_2C_2tBu_2$)] (1)

A yellow-brown suspension of [Cp*$RhCl_2$]$_2$ (170 mg, 0.28 mmol, 0.5 equiv.) in toluene (6 mL) was added to a brown-red solution of [Co(η^4-$P_2C_2tBu_2SiMe_3$)(η^4-$P_2C_2tBu_2$)] (293 mg, 0.55 mmol, 1.0 eq) in toluene (10 mL). The reaction mixture was stirred for 18 hours whereupon the color changed from dark-red to olive-green. The solvent was removed and the brown residue was dried *in vacuo*. The $^{31}P\{^1H\}$ NMR spectrum of the crude reaction solution is shown in Figure S5. The residue was purified by column chromatography (20 x 2 cm^2) with pre-dried Alumina N and *n*-hexane as eluent. The green band was collected. Subsequently, the solvent was removed and the olive-green residue was washed with toluene to afford pure [Co_2(η^4-$P_2C_2tBu_2$)$_2$(μ:η^4:η^4-$P_2C_2tBu_2$)].

Crystals suitable for X-ray diffraction were obtained by slow evaporation of an *n*-hexane solution.

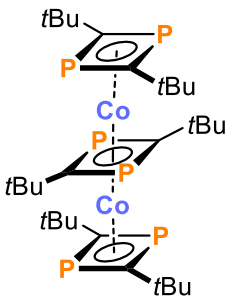

$C_{30}H_{54}Co_2P_6$, MW = 718.47 g·mol^{-1}

Yield 34 mg (17%)

^{1}H NMR (400.13 MHz, [D_8]THF, 300 K) δ = 1.33 (s, 18H, *t*Bu), 1.37 (s, 36H, *t*Bu) ppm.

$^{13}C\{^1H\}$ NMR (100.61 MHz, [D_8]THF, 300 K) δ = 31.9 (s, C(CH_3)$_3$, terminal $P_2C_2tBu_2$), 37.2 (t, J_{CP} = 7.2 Hz, C(CH_3)$_3$, terminal $P_2C_2tBu_2$), 38.4 (t, J_{CP} = 4.3 Hz, C(CH_3)$_3$, bridging $P_2C_2tBu_2$), 40.4 (s, C(CH_3)$_3$, bridging $P_2C_2tBu_2$), 113.4 (terminal $P_2C_2tBu_2$, assigned by ^1H-^{13}C-HMBC), 116.8 (bridging $P_2C_2tBu_2$, assigned by ^1H-^{13}C-HMBC) ppm.

$^{31}P\{^1H\}$ NMR (161.98 MHz, [D_8]THF, 300 K) δ = 55.8 (s, 4P), 111.1 (s, 2P) ppm.

UV/Vis (THF, λ_{max} /nm, (ε_{max} /L·mol^{-1}·cm^{-1})): 403 (67700), 502 (shoulder), 635 (3300).

LIFDI-MS m/z = 718.17, M^+ (calc. 718.13).

Elemental Analysis calcd. for $C_{30}H_{54}Co_2P_6$: C 50.15, H 7.58; found C 50.44, H 7.60.

3 Characterization of [$Co_2(\eta^4$-$P_2C_2tBu_2)_2(\mu$:η^4:η^4-$P_2C_2tBu_2)$] (1)

3.1 NMR Spectra

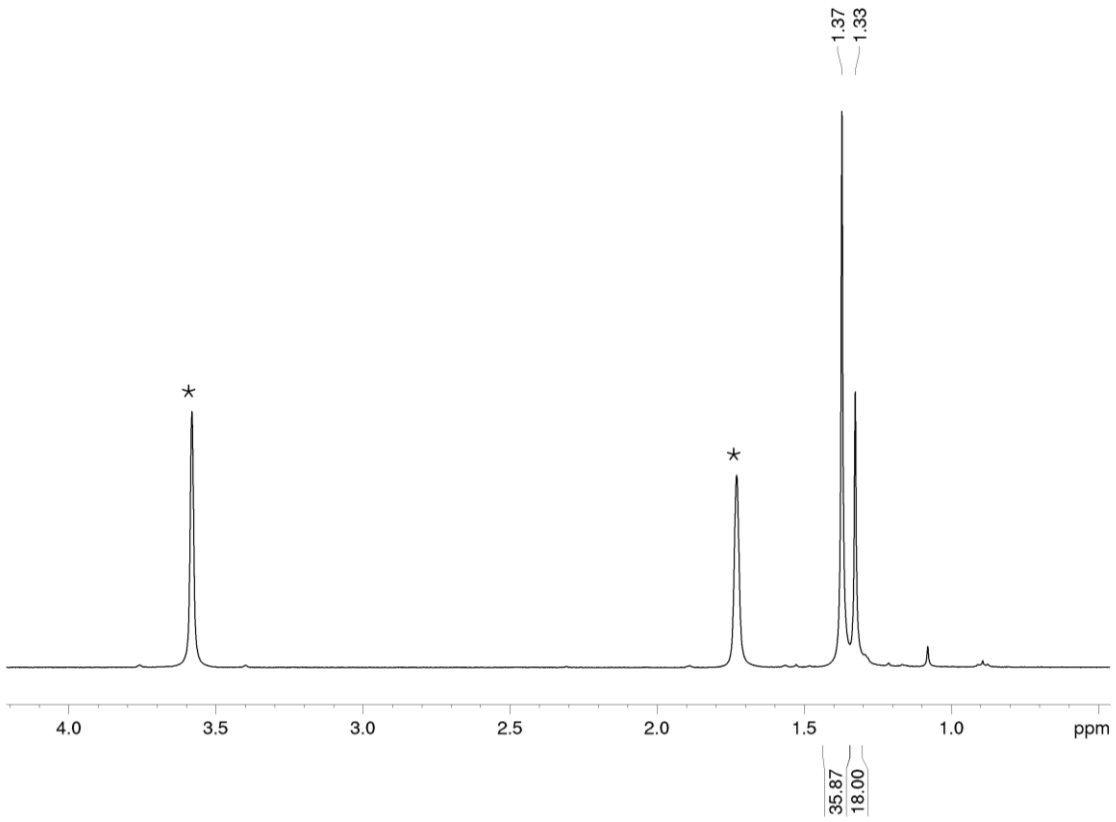

Figure S1. ^1H NMR spectrum (400.13 MHz, [D_8]THF, 300 K) of [$Co_2(\eta^4$-$P_2C_2tBu_2)_2(\mu$:η^4:η^4-$P_2C_2tBu_2)$] (**1**); * = [D_8]THF.

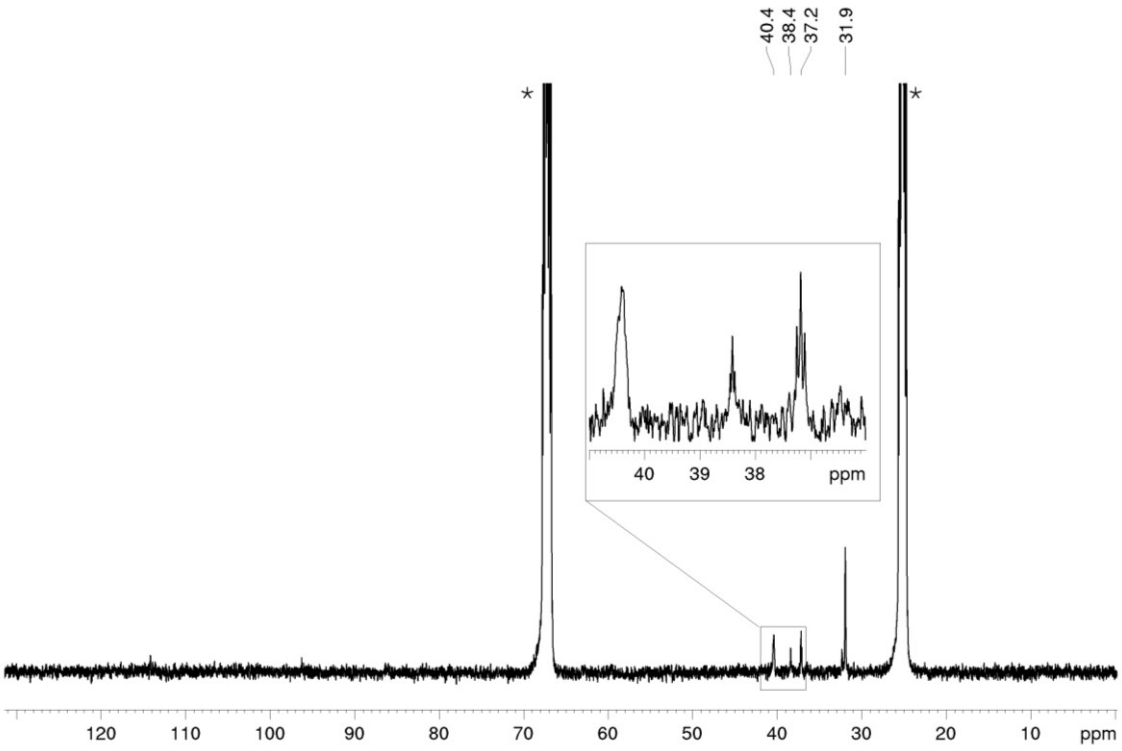

Figure S2. $^{13}C\{^{1}H\}$ NMR spectrum (100.61 MHz, $[D_8]THF$, 300 K) of $[Co_2(\eta^4\text{-}P_2C_2tBu_2)_2(\mu\text{:}\eta^4\text{:}\eta^4\text{-}P_2C_2tBu_2)]$ (**1**). * = $[D_8]THF$.

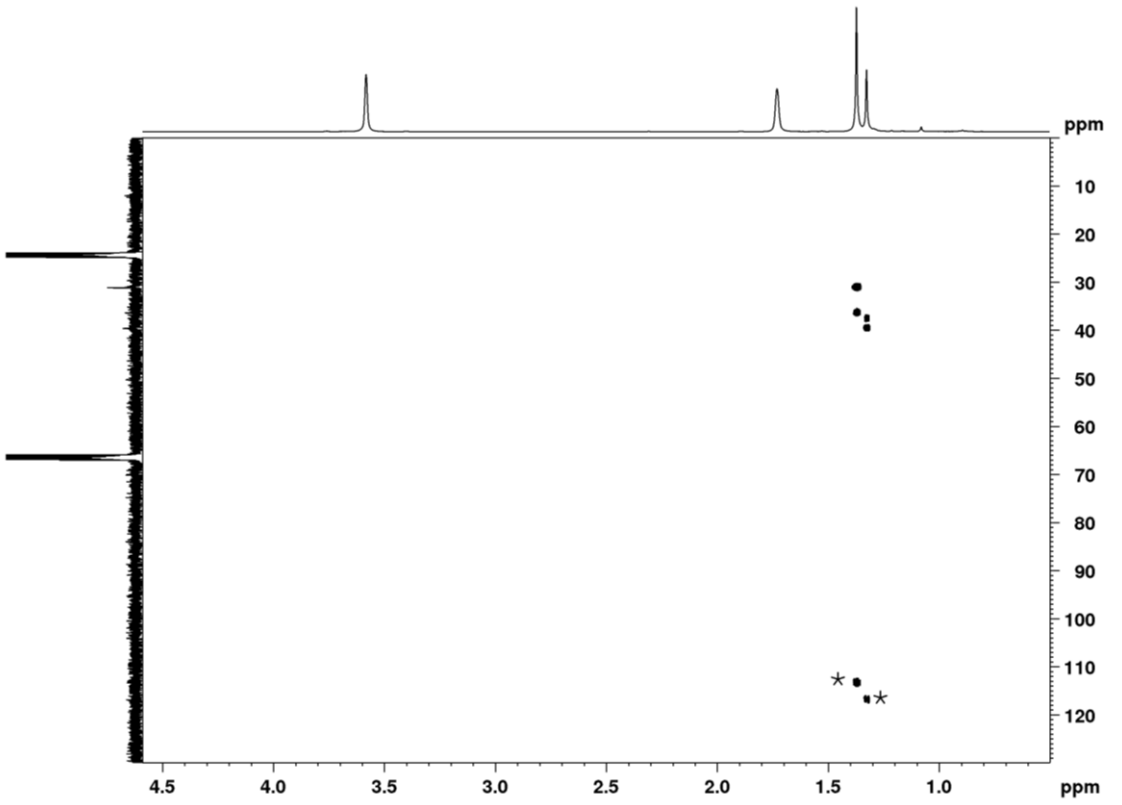

Figure S3. $^{1}H\text{-}^{13}C$-HMBC NMR spectrum (100.61 MHz/400.14 MHz, $[D_8]THF$, 300 K) of $[Co_2(\eta^4\text{-}P_2C_2tBu_2)_2(\mu\text{:}\eta^4\text{:}\eta^4\text{-}P_2C_2tBu_2)]$ (**1**), * = signals corresponding to correlation between protons and the carbon of the diphosphacyclobutadiene rings, which were not detected in the $^{13}C\{^{1}H\}$ NMR spectrum.

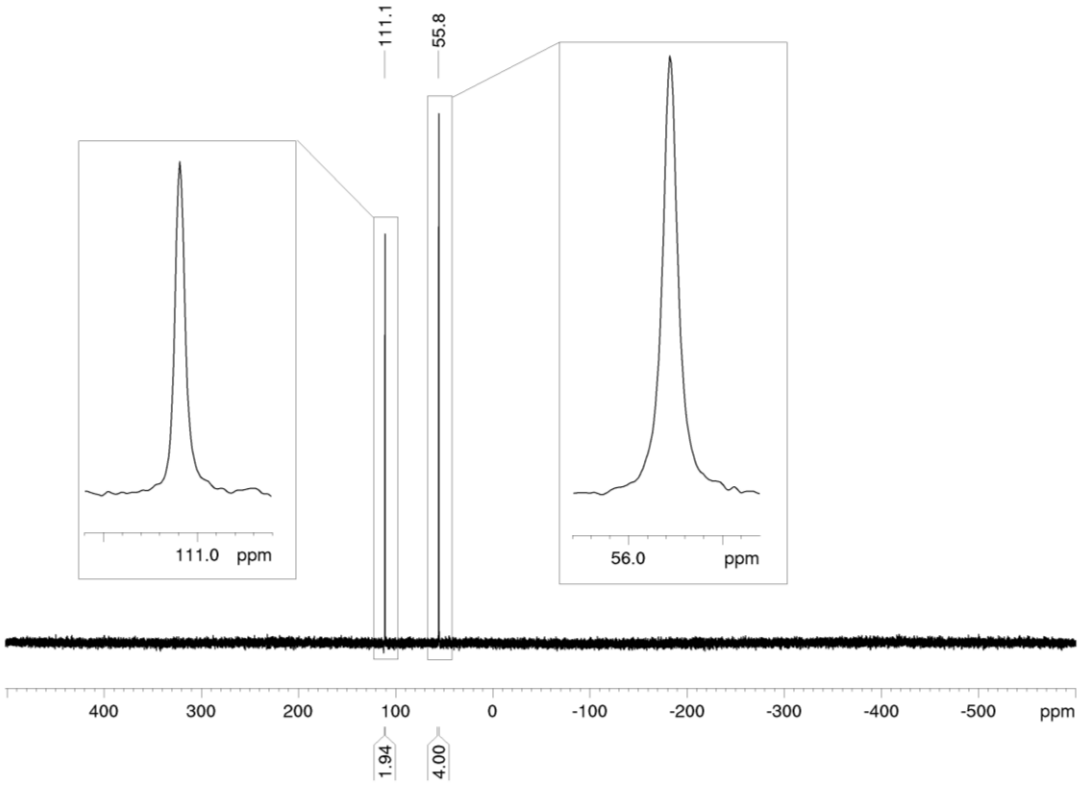

Figure S4. $^{31}P\{^{1}H\}$ NMR spectrum (161.98 MHz, [D_8]THF, 300 K) of $[Co_2(\eta^4\text{-}P_2C_2t\text{Bu}_2)_2(\mu\text{:}\eta^4\text{:}\eta^4\text{-}P_2C_2t\text{Bu}_2)]$ (**1**).

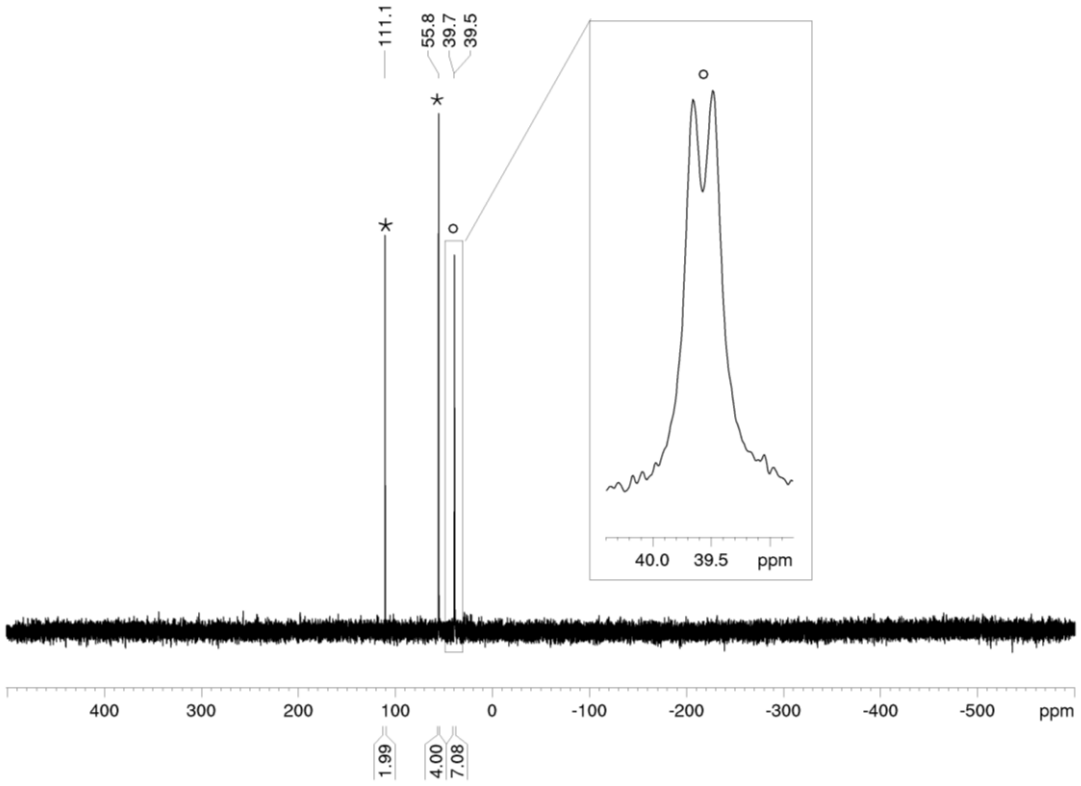

Figure S5. $^{31}P\{^{1}H\}$ NMR spectrum (161.98 MHz, [D_8]THF, 300 K) of the crude reaction mixture from the reaction of $[Co(\eta^4\text{-}P_2C_2t\text{Bu}_2\text{SiMe}_3)(\eta^4\text{-}P_2C_2t\text{Bu}_2)]$ with $[Cp^*RhCl_2]_2$; * = $[Co_2(\eta^4\text{-}P_2C_2t\text{Bu}_2)_2(\mu\text{:}\eta^4\text{:}\eta^4\text{-}P_2C_2t\text{Bu}_2)]$ (**1**); ° = $[Cp^*Rh(P_2C_2t\text{Bu}_2)]$.

3.2 UV/Vis Absorption Spectrum

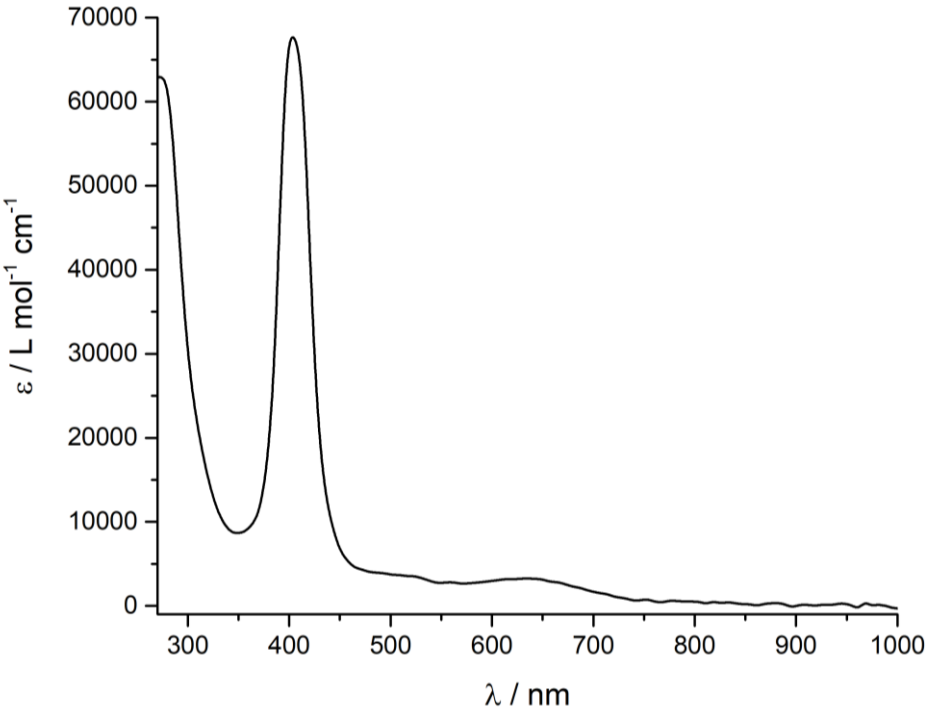

Figure S6. UV/Vis spectrum of $[Co_2(\eta^4\text{-}P_2C_2t\text{Bu}_2)_2(\mu\text{:}\eta^4\text{:}\eta^4\text{-}P_2C_2t\text{Bu}_2)]$ (**1**) in THF.

3.3 Mass Spectrometry

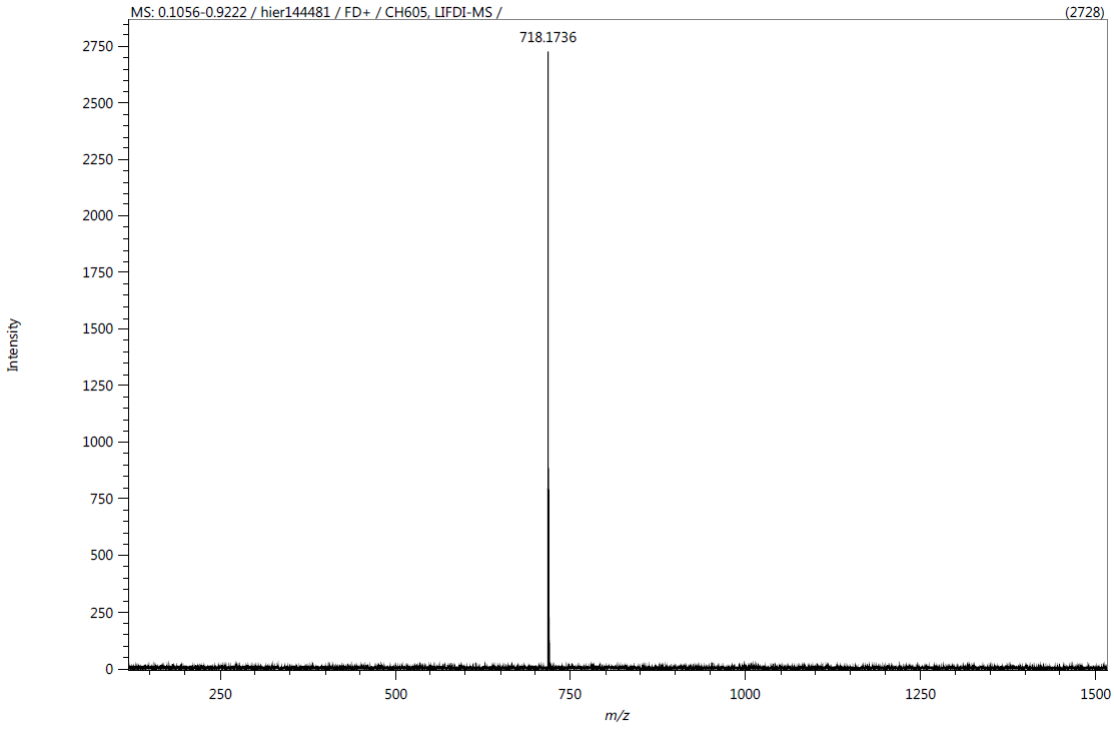

Figure S7. Mass spectrum of $[Co_2(\eta^4\text{-}P_2C_2t\text{Bu}_2)_2(\mu\text{:}\eta^4\text{:}\eta^4\text{-}P_2C_2t\text{Bu}_2)]$ (**1**).

3.4 Cyclic Voltammetry

Cyclic voltammetry experiments were performed in a single-compartment cell inside a nitrogen-filled glovebox using a CH Instruments CHI600E potentiostat. The cell was equipped with a platinum disc working electrode (2 mm diameter) polished with 0.05 µm alumina paste, a platinum wire counter electrode and a silver/silver nitrate reference electrode. The supporting electrolyte, tetra-*n*-butylammonium hexafluorophosphate, was dried in vacuo at 110 °C for three days. All redox potentials are reported versus the ferrocene/ferrocenium (Fc/Fc^+) couple. The scan rate is v = 100 mV s^{-1}. In the experimental setup, 4 mg of complex **1** and 100 mg of [^{n}Bu$_4$N][PF_6] were dissolved in 5 ml of THF.

3.5 X-ray Crystallography

The single crystal X-ray diffraction data was recorded on an Agilent Technologies SuperNova diffractometer with Cu K_α radiation (λ = 1.54184 Å). Crystals were selected under mineral oil, mounted on micromount loops and quench-cooled using an Oxford Cryosystems open flow N_2 cooling device. Either semi-empirical multi-scan absorption corrections[2,3] or analytical ones[4] were applied to the data. The structures were solved with SHELXT[5] solution program using dual methods and by using Olex2 as the graphical interface.[6] The models were refined with ShelXL[7] using full matrix least squares minimization on F^2.[8] The hydrogen atoms were located in idealized positions and refined isotropically with a riding model.

Crystallographic data for the structure of **1** have been deposited with the Cambridge Crystallographic Data Centre, CCDC, 12 Union Road, Cambridge CB21EZ, UK. Copies of these data can be obtained free of charge (http://www.ccdc.cam.ac.uk) on quoting the depository number 2195221.

Table S1. Crystal and structure refinement data of $[Co_2(\eta^4\text{-}P_2C_2tBu_2)_2(\mu{:}\eta^4{:}\eta^4\text{-}P_2C_2tBu_2)]$ (**1**).

Compound	**1**
Empirical formula	$C_{30}H_{54}Co_2P_6$
Formula weight	718.41
Temperature [K]	123(1)
Crystal system	monoclinic
Space group	$P2_1/n$
a [Å]	9.9927(3)
b [Å]	17.6107(5)
c [Å]	10.2590(3)
α [°]	90
β [°]	108.105(4)
γ [°]	90
Volume [Å^3]	1716.0(1)
Z	2
ρ_{calc} [g/cm^3]	1.390
μ [mm^{-1}]	10.351
F(000)	756.0
Crystal size [mm^3]	0.169 × 0.081 × 0.036
Radiation	CuK_α (λ = 1.54184)
2Θ range for data collection [°]	10.046 to 149.084
Index ranges	−12 ≤ h ≤ 12, −22 ≤ k ≤ 21, −8 ≤ l ≤ 12
Reflections collected	21151
Independent reflections	3481 [R_{int} = 0.0485, R_{sigma} = 0.0294]
Data / restraints / parameters	3841 / 0 / 181
Goodness-of-fit on F^2	1.122
Final R indexes [I>=2σ (I)]	R_1 = 0.0339, wR_2 = 0.0879
Final R indexes [all data]	R_1 = 0.0366, wR_2 = 0.0898
Largest diff. peak/hole [e Å^{-3}]	0.55/−0.27
CCDC deposition number	2195221

4 Quantum Chemical Calculations

Geometry optimization of **1** was performed with the Gaussian09 program package (Revision E.01).[9] The BP86 density functional[10] and the Ahlrichs def2-TZVP basis set[12] were employed for all atoms. Atom-pairwise dispersion correction to the DFT energy with Becke–Johnson damping (D3BJ) was applied.[11] Unless noted otherwise, all calculations were performed using the restricted DFT formalism. The nature of the optimized singlet state was verified by numerical frequency analyses. The optimized geometry of **1** in a triplet spin state is very similar to that of the singlet state with the difference that the P-Co distances to the end-decks are slightly longer. This is in line with the population of the SOMO-1 orbital which is Co-P antibonding (see Figure S12 below). The triplet state lies energetically 20 kcal/mol higher than the singlet state.

TD-DFT calculations were carried out at the B3LYP/def2-TZVP[12,13] level using the xyz coordinates of the optimized structure. Tetrahydrofuran solvent effects were considered by applying the SCRF method as implemented in Gaussian.[14] Molecular orbitals were visualized with the program GaussView5.[15] The isosurface value is set to 0.05 for all figures unless noted otherwise. DFT optimision of the triplet state indicated

Intrinsic bond orbital calculations were performed with the ORCA program package[16] in the gas phase on the BP86-D3BJ/def2-TZVP level of theory.[12,13] The RI[17] approximation was used. Intrinsic bond orbitals (IBOs) have been constructed from the occupied BP86 orbitals according to Knizia *et al*.[18] The results were visualized using Chemcraft (Figure S9).[19]

Table S2. Optimized Cartesian coordinates of **1** (singlet spin state).

1	Co	0.019216	1.740705	0.000000
2	P	0.000000	0.000000	1.446757
3	P	1.330544	3.620670	0.000000
4	P	-1.394988	3.514828	0.000000
5	C	-0.022733	3.468148	-1.168741
6	C	-1.196493	0.023299	-0.000000
7	C	0.033064	3.619502	-2.666677
8	C	-0.022733	3.468148	1.168741
9	C	-2.730466	0.112299	0.000000
10	C	0.033064	3.619502	2.666677
11	C	1.337140	3.013435	-3.215677
12	H	2.217769	3.463552	-2.731138
13	H	1.418257	3.192914	-4.298356
14	H	1.363472	1.928383	-3.040918
15	C	-3.205736	0.847932	1.265488
16	H	-2.845970	0.335922	2.171753
17	H	-4.305292	0.863336	1.300978
18	H	-2.844930	1.882388	1.285163

19	C	0.020749	5.140837	-2.954970
20	H	-0.900614	5.601860	-2.569561
21	H	0.074808	5.322740	-4.039582
22	H	0.877807	5.635491	-2.474503
23	C	-3.205736	0.847932	-1.265488
24	H	-2.844930	1.882388	-1.285163
25	H	-4.305292	0.863336	-1.300978
26	H	-2.845970	0.335922	-2.171753
27	C	-1.175254	2.968048	3.356374
28	H	-2.121316	3.364929	2.958033
29	H	-1.151784	3.171507	4.437778
30	H	-1.167588	1.879269	3.210290
31	C	-1.175254	2.968048	-3.356374
32	H	-1.167588	1.879269	-3.210290
33	H	-1.151784	3.171507	-4.437778
34	H	-2.121316	3.364929	-2.958033
35	C	0.020749	5.140837	2.954970
36	H	0.877807	5.635491	2.474503
37	H	0.074808	5.322740	4.039582
38	H	-0.900614	5.601860	2.569561
39	C	1.337140	3.013435	3.215677
40	H	1.363472	1.928383	3.040918
41	H	1.418257	3.192914	4.298356
42	H	2.217769	3.463552	2.731138
43	C	-3.431834	-1.255144	-0.000000
44	H	-3.170812	-1.843322	-0.888157
45	H	-4.521648	-1.096620	-0.000000
46	H	-3.170812	-1.843322	0.888157
47	P	0.000000	0.000000	-1.446757
48	C	1.196493	-0.023299	-0.000000
49	C	2.730466	-0.112299	0.000000
50	C	3.205736	-0.847932	-1.265488
51	H	2.845970	-0.335922	-2.171753
52	H	4.305292	-0.863336	-1.300978
53	H	2.844930	-1.882388	-1.285163
54	C	3.205736	-0.847932	1.265488
55	H	2.844930	-1.882388	1.285163
56	H	4.305292	-0.863336	1.300978
57	H	2.845970	-0.335922	2.171753
58	C	3.431834	1.255144	-0.000000
59	H	3.170812	1.843322	0.888157
60	H	4.521648	1.096620	-0.000000
61	H	3.170812	1.843322	-0.888157
62	Co	-0.019216	-1.740705	0.000000
63	P	-1.330544	-3.620670	0.000000
64	P	1.394988	-3.514828	0.000000
65	C	0.022733	-3.468148	1.168741
66	C	-0.033064	-3.619502	2.666677
67	C	0.022733	-3.468148	-1.168741
68	C	-0.033064	-3.619502	-2.666677
69	C	-1.337140	-3.013435	3.215677
70	H	-2.217769	-3.463552	2.731138
71	H	-1.418257	-3.192914	4.298356
72	H	-1.363472	-1.928383	3.040918
73	C	-0.020749	-5.140837	2.954970
74	H	0.900614	-5.601860	2.569561

75	H	-0.074808	-5.322740	4.039582
76	H	-0.877807	-5.635491	2.474503
77	C	1.175254	-2.968048	-3.356374
78	H	2.121316	-3.364929	-2.958033
79	H	1.151784	-3.171507	-4.437778
80	H	1.167588	-1.879269	-3.210290
81	C	1.175254	-2.968048	3.356374
82	H	1.167588	-1.879269	3.210290
83	H	1.151784	-3.171507	4.437778
84	H	2.121316	-3.364929	2.958033
85	C	-0.020749	-5.140837	-2.954970
86	H	-0.877807	-5.635491	-2.474503
87	H	-0.074808	-5.322740	-4.039582
88	H	0.900614	-5.601860	-2.569561
89	C	-1.337140	-3.013435	-3.215677
90	H	-1.363472	-1.928383	-3.040918
91	H	-1.418257	-3.192914	-4.298356
92	H	-2.217769	-3.463552	-2.731138

Table S3. Optimized Cartesian coordinates of **1** (triplet spin state).

Co	0.025451000	1.769346000	0.000000000
P	0.000000000	0.000000000	1.443121000
P	1.348908000	3.686039000	0.000000000
P	-1.405856000	3.589497000	0.000000000
C	-0.019186000	3.512025000	-1.160037000
C	-1.196426000	0.018916000	0.000000000
C	0.031469000	3.649870000	-2.659392000
C	-0.019186000	3.512025000	1.160037000
C	-2.728941000	0.110154000	0.000000000
C	0.031469000	3.649870000	2.659392000
C	1.327369000	3.032104000	-3.213704000
H	2.214155000	3.470776000	-2.730145000
H	1.405779000	3.214686000	-4.295920000
H	1.344193000	1.945972000	-3.043089000
C	-3.205023000	0.846228000	1.265483000
H	-2.847394000	0.334896000	2.172805000
H	-4.304561000	0.858432000	1.297662000
H	-2.844117000	1.880657000	1.281890000
C	0.029339000	5.171476000	-2.953917000
H	-0.884186000	5.641799000	-2.561629000
H	0.072536000	5.342977000	-4.040533000
H	0.896905000	5.660224000	-2.487067000
C	-3.205023000	0.846228000	-1.265483000
H	-2.844117000	1.880657000	-1.281890000
H	-4.304561000	0.858432000	-1.297662000
H	-2.847394000	0.334896000	-2.172805000
C	-1.187568000	3.007666000	3.337888000
H	-2.126998000	3.417871000	2.937312000
H	-1.166242000	3.203456000	4.420588000
H	-1.191775000	1.920176000	3.183505000
C	-1.187568000	3.007666000	-3.337888000
H	-1.191775000	1.920176000	-3.183505000
H	-1.166242000	3.203456000	-4.420588000

H	-2.126998000	3.417871000	-2.937312000
C	0.029339000	5.171476000	2.953917000
H	0.896905000	5.660224000	2.487067000
H	0.072536000	5.342977000	4.040533000
H	-0.884186000	5.641799000	2.561629000
C	1.327369000	3.032104000	3.213704000
H	1.344193000	1.945972000	3.043089000
H	1.405779000	3.214686000	4.295920000
H	2.214155000	3.470776000	2.730145000
C	-3.430790000	-1.258534000	0.000000000
H	-3.165417000	-1.845259000	-0.887644000
H	-4.520280000	-1.097488000	0.000000000
H	-3.165417000	-1.845259000	0.887644000
P	0.000000000	0.000000000	-1.443121000
C	1.196426000	-0.018916000	0.000000000
C	2.728941000	-0.110154000	0.000000000
C	3.205023000	-0.846228000	-1.265483000
H	2.847394000	-0.334896000	-2.172805000
H	4.304561000	-0.858432000	-1.297662000
H	2.844117000	-1.880657000	-1.281890000
C	3.205023000	-0.846228000	1.265483000
H	2.844117000	-1.880657000	1.281890000
H	4.304561000	-0.858432000	1.297662000
H	2.847394000	-0.334896000	2.172805000
C	3.430790000	1.258534000	0.000000000
H	3.165417000	1.845259000	0.887644000
H	4.520280000	1.097488000	0.000000000
H	3.165417000	1.845259000	-0.887644000
Co	-0.025451000	-1.769346000	0.000000000
P	-1.348908000	-3.686039000	0.000000000
P	1.405856000	-3.589497000	0.000000000
C	0.019186000	-3.512025000	1.160037000
C	-0.031469000	-3.649870000	2.659392000
C	0.019186000	-3.512025000	-1.160037000
C	-0.031469000	-3.649870000	-2.659392000
C	-1.327369000	-3.032104000	3.213704000
H	-2.214155000	-3.470776000	2.730145000
H	-1.405779000	-3.214686000	4.295920000
H	-1.344193000	-1.945972000	3.043089000
C	-0.029339000	-5.171476000	2.953917000
H	0.884186000	-5.641799000	2.561629000
H	-0.072536000	-5.342977000	4.040533000
H	-0.896905000	-5.660224000	2.487067000
C	1.187568000	-3.007666000	-3.337888000
H	2.126998000	-3.417871000	-2.937312000
H	1.166242000	-3.203456000	-4.420588000
H	1.191775000	-1.920176000	-3.183505000
C	1.187568000	-3.007666000	3.337888000
H	1.191775000	-1.920176000	3.183505000
H	1.166242000	-3.203456000	4.420588000
H	2.126998000	-3.417871000	2.937312000
C	-0.029339000	-5.171476000	-2.953917000
H	-0.896905000	-5.660224000	-2.487067000
H	-0.072536000	-5.342977000	-4.040533000
H	0.884186000	-5.641799000	-2.561629000
C	-1.327369000	-3.032104000	-3.213704000

H	-1.344193000	-1.945972000	-3.043089000
H	-1.405779000	-3.214686000	-4.295920000
H	-2.214155000	-3.470776000	-2.730145000

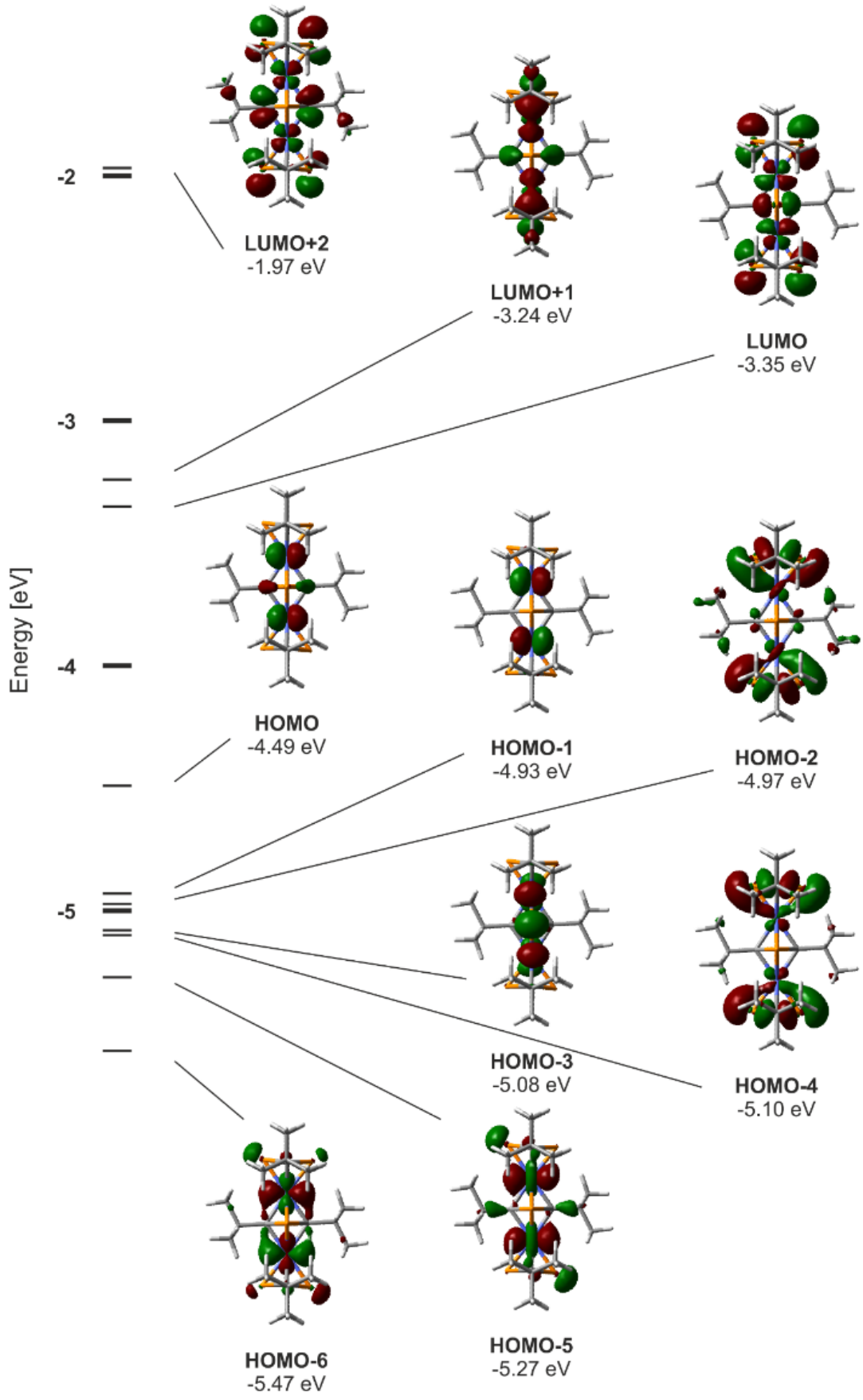

Figure S8. Kohn-Sham frontier orbitals of $[Co_2(\eta^4\text{-}P_2C_2t\text{Bu}_2)_2(\mu\text{:}\eta^4\text{:}\eta^4\text{-}P_2C_2t\text{Bu}_2)]$ (**1**) calculated at the BP86-D3BJ/def2-TZVP level of theory.

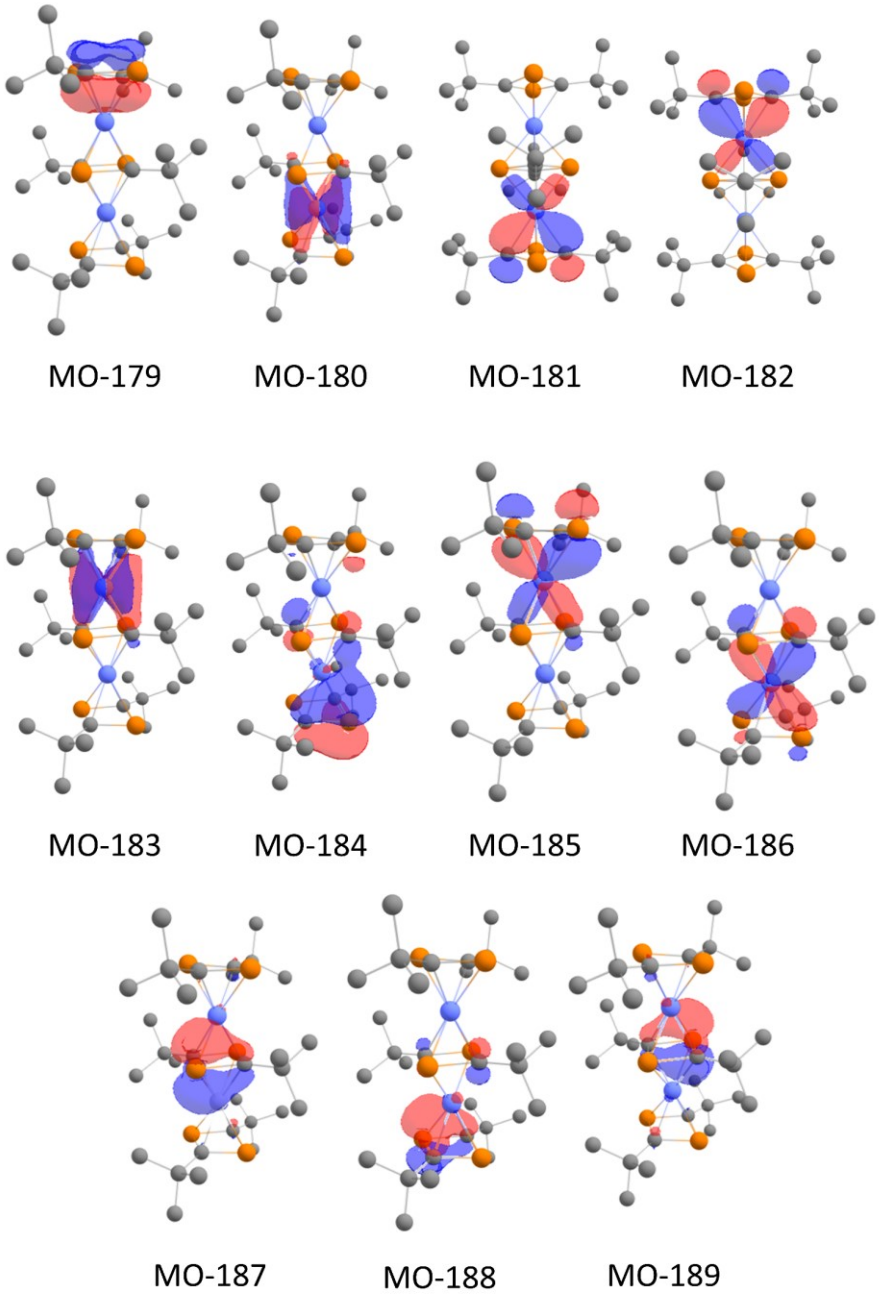

Figure S9. Intrinsic Bond Orbitals (IBOs) of $[Co_2(\eta^4\text{-}P_2C_2t\text{Bu}_2)_2(\mu\text{:}\eta^4\text{:}\eta^4\text{-}P_2C_2t\text{Bu}_2)]$ (**1**) calculated at the BP86-D3BJ/def2-TZVP level of theory displaying multicenter bonds.

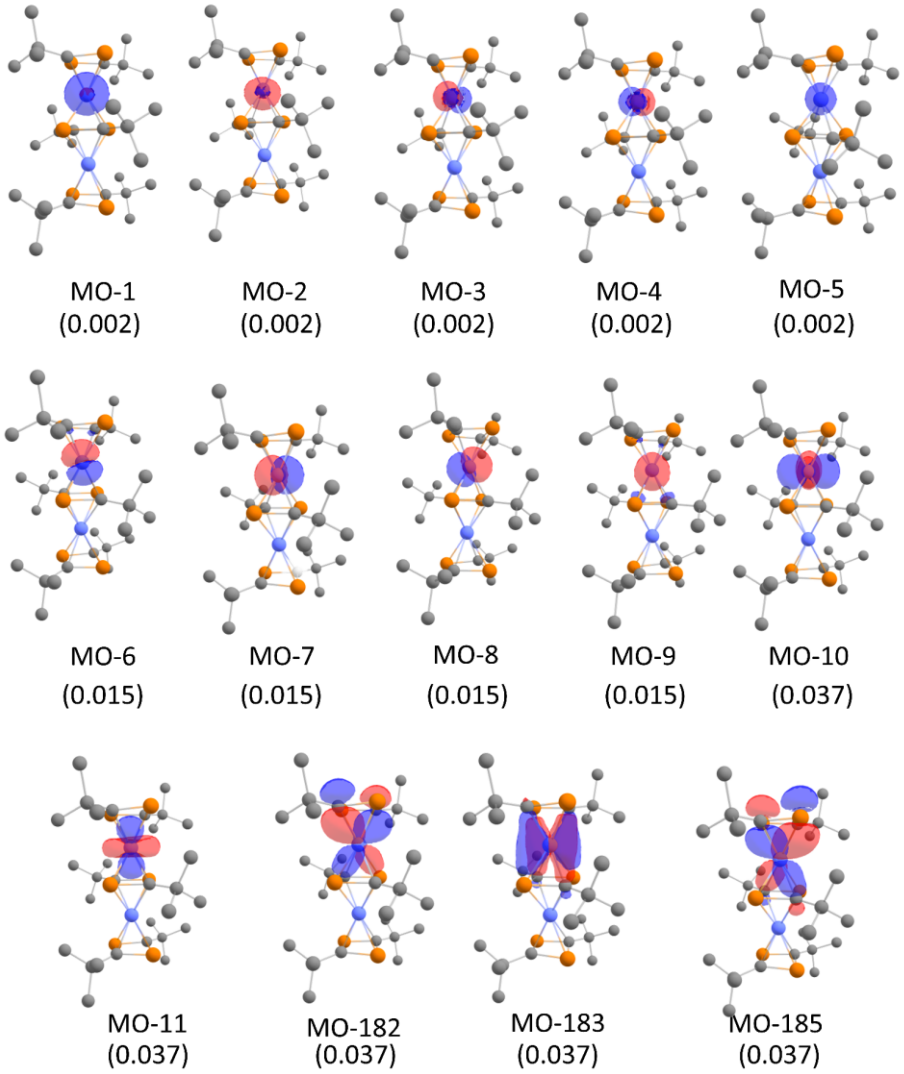

Figure S10. Intrinsic Bond Orbitals (IBOs) of $[Co_2(\eta^4\text{-}P_2C_2t\text{Bu}_2)_2(\mu\text{:}\eta^4\text{:}\eta^4\text{-}P_2C_2t\text{Bu}_2)]$ (**1**) calculated at the BP86-D3BJ/def2-TZVP level of theory showing populated orbitals with Co-contribution. Isosurface values are given in brackets.

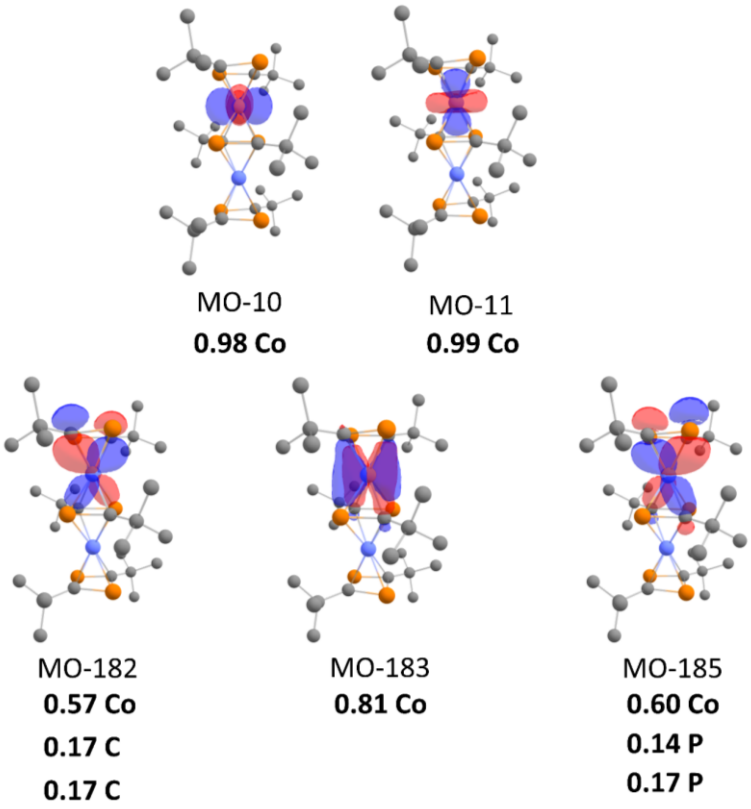

Figure S11. Intrinsic Bond Orbitals (IBOs) of [$Co_2(\eta^4\text{-}P_2C_2t\text{Bu}_2)_2(\mu\text{:}\eta^4\text{:}\eta^4\text{-}P_2C_2t\text{Bu}_2)$] (**1**) calculated at the BP86-D3BJ/def2-TZVP level of theory showing populated d-orbitals with Co-contribution. Bold values below the orbitals show the contributions of atoms.

Inspection of the Intrinsic Bond Orbitals (IBOs) involving cobalt atoms (Figure S10 and Figure S11) reveal 14 molecular orbitals with significant contributions of the Co-atoms. While the s- and p-orbitals are strongly localized on the Co atoms, some of the d-orbitals (Figure S11, MOs 10, 11, 182, 183 and 185) show highly covalent interactions (MOs 182 and 185). With cobalt contributions of 0.57 and 0.60 and significant covalent interactions with the $P_2C_2t\text{Bu}_2$ ligands. Furthermore, Mulliken population analysis reveals an atomic population of the Co atoms with 27.82 electrons each, formally corresponding to a Co(-I) oxidation state. The sum of the Mulliken gross atomic charges of the phosphorus and carbon atoms of the diphosphacyclobutadiene ligands are positive (0.43 for terminal and 0.72 for bridging P_2C_2). In conclusion, a definitive assignment of charges and oxidation state is not easily possible due to highly covalent interactions between the Co and the P_2C_2 ligands, which necessarily render an oxidation state assignment ambiguous. Note that very similar observations have been made on closely related bis(diphosphacyclobutadiene)cobalt complexes, for which the problem of oxidation state assignement has been discussed exhaustively.[20]

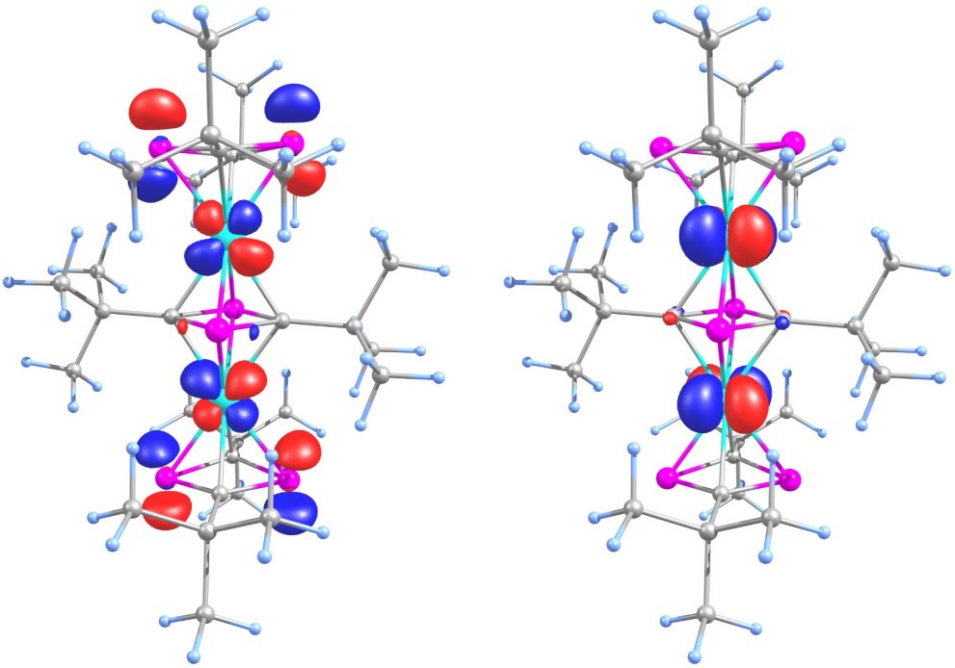

Figure S12. Singly occupied Kohn-Sham frontier orbitals of [$Co_2(\eta^4\text{-}P_2C_2t\text{Bu}_2)_2(\mu\text{:}\eta^4\text{:}\eta^4\text{-}P_2C_2t\text{Bu}_2)$] (**1**) in the triplet spin state, calculated at the BP86-D3BJ/def2-TZVP level of theory. Left: SOMO-1 (-4.529 eV), Right: SOMO (-3.324 eV)

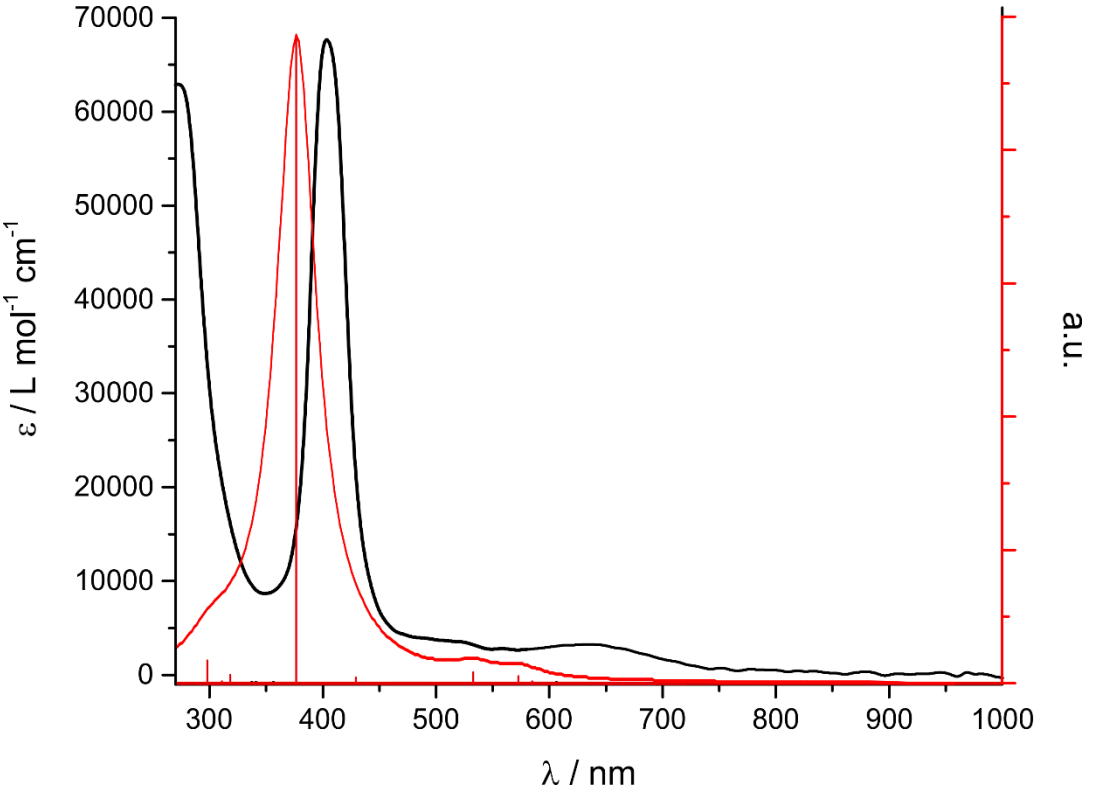

Figure S13. Experimental (black) and calculated (red) UV/Vis spectrum of [$Co_2(\eta^4\text{-}P_2C_2t\text{Bu}_2)_2(\mu\text{:}\eta^4\text{:}\eta^4\text{-}P_2C_2t\text{Bu}_2)$] (**1**) in THF (a.u. = arbitrary units).

Table S4. Calculated electronic transitions of [$Co_2(\eta^4\text{-}P_2C_2t\text{Bu}_2)_2(\mu{:}\eta^4{:}\eta^4\text{-}P_2C_2t\text{Bu}_2)$] (**1**) on the B3LYP/def2-TZVP level of theory. The corresponding molecular orbitals are shown in Figure S8.

#	*v* [nm]	*f*	%	Transition	Exp. *v* [nm]	Difference Exp. / Calc *v*
1	572	0.011	20	HOMO−9 → LUMO+2	635	63 nm
			45	HOMO−8 → LUMO		1734 cm^{-1}
			29	HOMO → LUMO		
2	532	0.014	19	HOMO−5 → LUMO	635	103
			62	HOMO → LUMO		3049 cm^{-1}
3	375	0.876	40	HOMO−6 → LUMO	403	28
			39	HOMO−4 → LUMO+1		1853 cm^{-1}
			15	HOMO → LUMO		

5 References

1 C. Rödl, J. Bissmeyer neè Malberg, R. Wolf, *Z. Naturforsch. B*, 2018, **76**, 895.

2 Sheldrick, G. M. SADABS, Bruker AXS, Madison, USA, 2007.

3 CrysAlisPro, Scale3 Abspack, Rigaku Oxford Diffraction, 2019.

4 R. C. Clark and J. S. Reid, *Acta Cryst. A*, 1995, **51**, 887.

5 G. M. Sheldrick, *Acta Cryst. A*, 2015, **71**, 3.

6 O. V. Dolomanov, L. J. Bourhis, R. J. Gildea, J. A. K. Howard and H. Puschmann, *J. Appl. Crystallogr.*, 2009, **42**, 339.

7 G. M. Sheldrick, *Acta Cryst. C*, 2015, **71**, 3.

8 G. M. Sheldrick, *Acta Cryst. A*, 2008, **64**, 112

9 Gaussian 09, Revision E.01: M. J. Frisch, G. W. Trucks, H. B. Schlegel, G. E. Scuseria, M. A. Robb, J. R. Cheeseman, G. Scalmani, V. Barone, G. A. Petersson, H. Nakatsuji, X. Li, M. Caricato, A. Marenich, J. Bloino, B. G. Janesko, R. Gomperts, B. Mennucci, H. P. Hratchian, J. V. Ortiz, A. F. Izmaylov, J. L. Sonnenberg, D. Williams-Young, F. Ding, F. Lipparini, F. Egidi, J. Goings, B. Peng, A. Petrone, T. Henderson, D. Ranasinghe, V. G. Zakrzewski, J. Gao, N. Rega, G. Zheng, W. Liang, M. Hada, M. Ehara, K. Toyota, R. Fukuda, J. Hasegawa, M. Ishida, T. Nakajima, Y. Honda, O. Kitao, H. Nakai, T. Vreven, K. Throssell, J. A. Montgomery, Jr., J. E. Peralta, F. Ogliaro, M. Bearpark, J. J. Heyd, E. Brothers, K. N. Kudin, V. N. Staroverov, T. Keith, R. Kobayashi, J. Normand, K. Raghavachari, A. Rendell, J. C. Burant, S. S. Iyengar, J. Tomasi, M. Cossi, J. M. Millam, M. Klene, C. Adamo, R. Cammi, J. W. Ochterski, R. L. Martin, K. Morokuma, O. Farkas, J. B. Foresman, and D. J. Fox, Gaussian, Inc., Wallingford CT, 2016.

10 a) A. D. Becke, *Phys. Rev. A* **1988**, *38*, 3098; b) J. P. Perdew, *Phys. Rev. B* **1986**, *33*, 8822.

11 a) S. Grimme, S. Ehrlich, L. Goerigk, *J. Comput. Chem.* **2011**, *32*, 1456. b) S. Grimme, J. Antony, S. Ehrlich, H. Krieg, *J. Chem. Phys.* **2010**, *132*, 154104.

12 a) A. Schäfer, C. Huber, R. Ahlrichs, *J. Chem. Phys.* **1994**, *100*, 5829; b) F. Weigend, *Phys. Chem. Chem. Phys*. **2006**, *8*, 1057.

13 a) C. Lee, W. Yang, R. G. Parr, *Phys. Rev. B* **1988**, *37*, 785; b) P. J. Stephens, F. J. Devlin, C. F. Chabalowski, M. J. Frisch, *J. Phys. Chem.* **1994**, *98*, 11623-11627.

14 J. Tomasi, B. Menucci, R. Cammi, *Chem. Rev.* **2005**, *105*, 2999-3093.

15 GaussView 5.0.9: R. Dennington, T. A. Keith, J. M. Millam, Semichem Inc., Shawnee Mission, KS, **2016**.

16 R. A. Kendall and H. A. Früchtl, *Theor. Chem. Acc.*, 1997, **97**, 158.

17 F. Weigend, *Phys. Chem. Chem. Phys.*, 2002, **4**, 4285.

18 G. Knizia, *J. Chem. Theory Comput.*, 2013, **9**, 4834.

19 Chemcraft - graphical software for visualisation of quantum chemistry computations. https://www.chemcraftprog.com.

20 R. Wolf, A. W. Ehlers, M. M. Khusniyarov, F. Hartl, B. de Bruin, G. J. Long, F. Grandjean, F. M. Schappacher, R. Pöttgen, J. C. Slootweg, M. Lutz, A. L. Spek, K. Lammertsma, *Chem. Eur. J.*, 2010, **16**, 14322−14334